The Effect of Cu Additions on the Precipitation Kinetics in an Al-Mg-Si Alloy with Excess Si

M. MURAYAMA, K. HONO, W.F. MIAO, and D.E. LAUGHLIN

The microstructural evolution during age hardening of a Cu-bearing Al-Mg-Si alloy has been investigated by the three-dimensional atom probe (3DAP) and transmission electron microscope (TEM) techniques, in order to clarify the effect of Cu on the initial age-hardening response. After 30 minutes of artificial aging at 175 °C, the alloy shows a significant increase in hardness. The TEM observations have revealed that very fine, needle-shaped β'' precipitates are formed in addition to spherical Guinier–Preston (GP) zones, whereas only the spherical GP zones are observed in the Al-Mg-Si ternary alloy using the same aging condition. The number density of the precipitates is significantly affected by the preaging conditions. The 3DAP analysis shows that the distribution of Cu atoms is uniform after 30 minutes of artificial aging at 175 °C, whereas Cu atoms are incorporated into the needle-shaped β'' precipitates after 10 hours of aging at 175 °C. Based on these microanalytical results, the effect of Cu additions on the age-hardening response of Al-Mg-Si alloys is discussed.

I. INTRODUCTION

THE 6000-series wrought Al-Mg-Si(-Cu) alloys are widely used as medium-strength structural alloys. In the continuing drive for automobile weight reduction, Al-Mg-Si(-Cu) alloys are considered to be the most promising candidates for heat-treatable body sheet materials. Numerous investigations on the precipitation process,[1,2,3] the process of two-step aging,[4] and the effect of alloy composition on the age-hardening response[5,6] have been carried out. Since the alloys for body sheet applications must be age hardened during the paint-baking process, substantial age hardening must occur during artificial aging for less than 30 minutes at about 175 °C. It has been reported that the Al-Mg-Si alloys containing excess amounts of Si, with respect to the Al-Mg_2Si quasibinary composition, exhibit a faster age-hardening response.[5] A recent atom-probe study by the present authors[7] revealed that the chemical compositions of the Guinier–Preston (GP) zones and the β'' precipitate change with the alloy composition, and that the number density of the GP zones in the paint-bake condition increases as the number of Si atoms available to form Mg-Si coclusters increases.

There are several reports on the effect of the quaternary-element addition on age hardening of Al-Mg-Si alloys.[1,8–10] Cu additions generally increase the kinetics of precipitation during artificial aging, as well as reduce the deterioration of the age-hardening response arising from natural aging of the Al-Mg-Si alloy. Collins[8] reported that the presence of Cu causes a small reduction in the solubility of Mg_2Si, which increases the supersaturation of the Mg_2Si phase for a given alloy composition. Chaterjee and Entwistle[9] reported that Cu reduces the rate of migration of Mg and Si atoms, which retards the formation of Mg-Si clusters at room temperature. They proposed that the smaller clusters are reverted at the temperature for artificial aging. This, in turn, increases the supersaturation of Mg_2Si, resulting in a larger driving force for precipitation at the temperature of artificial aging. Suzuki *et al.*[11] also reported that Cu additions increase the initial rate of hardening and the peak hardness. This was attributed to the increase in the number density of the needle-shaped precipitates with increasing Cu content. More recently, Laughlin *et al.*[10] reported that the Cu level has a large effect on the age-hardening kinetics in the underaged regime and a smaller but noticeable effect on the value of peak hardness. They found that the microstructure of the alloy with a higher Cu content is much finer than that of the alloy with a lower Cu content, as reported earlier by Pashley *et al.*[1] In addition, they attributed the increase of the kinetics of artificial aging to the formation of Q' precipitates, which form in addition to the phases that precipitate in the ternary alloys. The Q' phase is considered to be a precursor phase (coherent version) of the equilibrium Q phase ($Al_5Cu_2Mg_8Si_6$[6,9] and $Al_4CuMg_5Si_4$[10]). Sagalowicz *et al.*[12] also reported the presence of lath-shaped precipitates in the Al-Mg-Si alloy with 0.01 wt pct Cu and 0.7 wt pct Mn, which are believed to be a derivative phase of the Q phase. Earlier, Dumolt *et al.*[13] reported the formation of lath-shaped B' precipitates in the quaternary alloy aged for 8 hours at 180 °C and proposed that the precipitates were orthogonal or hexagonal, with the long dimension of the lath along the $\langle 100 \rangle_{Al}$ direction. This B' phase is the same as the Q' one reported later by Laughlin *et al.*[10] Edwards *et al.*[14] also reported the formation of B' (or Q', per Reference 10) in the commercial 6061 alloy. However, the Q' (or B') phase was reported only in overaged alloys. It has not been shown that this phase forms in the standard paint-bake condition (30 minutes of aging at 175 °C) of automotive applications.

Since the typical paint-bake cycle in the automobile manufacturing process is 30 minutes of heating at around 175 °C, the body sheet aluminum alloys are used in the underaged condition. It is, therefore, important to investigate the effect of Cu in the early stages of artificial aging. The aim of this

M. MURAYAMA, Researcher, and K. HONO, Head of 3rd Laboratory, are with the Materials Physics Division, National Research Institute for Metals, Tsukuba 305-0047, Japan. W.F. MIAO, formerly Postdoctoral Fellow with the Department of Materials Science and Engineering, Carnegie Mellon University, is with Nanomat, Inc., North Huntingdon, PA 15642. D.E. LAUGHLIN, Professor, is with the Department of Materials Science and Engineering, Carnegie Mellon University, Pittsburgh, PA 15213-3890.

Manuscript submitted September 8, 1999.

Table I. Chemical Compositions of the Alloys (Atomic Percent)

Specimen Code	Mg	Si	Cu	Fe	Mn	Al
0.4Cu	0.61	1.22	0.39	0.05	0.03	bal
0.0Cu	0.64	1.23	0.03	0.05	0.04	bal

study is to clarify the role of Cu additions to an Al-Mg-Si alloy in enhancing the age-hardening response. For this purpose, we attempted to clarify the chemical compositions of the precipitation products that form in Al-Mg-Si-Cu alloys after artificial aging at 175 °C, using a three-dimensional atom probe (3DAP) and a transmission electron microscope (TEM). The 3DAP is capable of mapping individual atoms in real space with a near-atomic resolution.[15,16] Thus, this technique can determine the chemical compositions of nanoscale precipitates embedded in a matrix phase without any convolution effect.

II. EXPERIMENTAL PROCEDURES

The chemical compositions of the alloys used in this study are listed in Table I. The alloys were solution treated at 550 °C for 30 minutes and subsequently water quenched. The solution-treated specimens were artificially aged for 30 minutes and 10 hours at 175 °C. In order to examine the effect of preaging, the specimens were aged at room temperature (natural aging), 70 °C, and 110 °C before artificial aging at 175 °C. The elemental distributions in the specimens were analyzed by a 3DAP equipped with the CAMECA tomographic atom-probe detection system.[16] The atom-probe analyses were carried out at about 30 K with a pulse fraction (V_p/V_{dc}) of 20 pct in UHV (a ultra high vacuum condition) ($\sim 1 \times 10^{-10}$ Torr). Needle-shaped specimens were produced using standard electropolishing with nitric acid solution. The microstructures of the samples were examined with a PHILIPS* CM 200 TEM operated at 200 kV. Thin foils for the TEM were prepared by grinding the slices to a thickness of about 100 μm, then by twin-jet electropolishing using a 33 pct nitric acid–methanol solution at −30 °C. In order to estimate the difference in the density of precipitates, TEM images were recorded from the area between the first and second thickness fringes, which guarantees that the areas studied in the samples had approximately equal thicknesses.

*PHILIPS is a trademark of Philips Electronic Instruments Corp. Mahwah, NJ.

III. RESULTS

The Vickers hardness measurements of the preaged and artificially aged specimens are shown in Figure 1. The value of the standard deviation (σ) is smaller than the size of the data points in Figure 1. The hardness of the specimens artificially aged for 30 minutes is influenced by the preaging conditions. However, the hardness of the 0.4Cu alloy aged for 10 hours has the same value regardless of the preaging conditions. In contrast, the hardness values of the 0.0Cu alloy aged for 10 hours after preaging at 70 °C and 110 °C become slightly larger than that of the directly aged specimen, whereas the peak hardness value of the naturally aged specimen becomes slightly smaller than that of directly aged one. This indicates that the preaging conditions do not influence the peak hardness of the 0.4Cu alloy, whereas they do influence the hardness in the paint-bake condition. In both alloys, the hardness values of the paint-bake condition become smaller when the specimen is preaged at room temperature, 70 °C, and 110 °C. This result indicates that the clusters formed during preaging do not enchance the precipitate hardening at 175 °C. This is in contrast to the case of the ternary alloy,[7] where preaging at 70 °C resulted in an increased number density of the precipitates in artificially aged specimens, whereas natural aging retarded the subsequent precipitation kinetics of artificial aging. It should be noted that the hardness of all the preaged 0.4Cu alloys, including the naturally aged one, are the same as the directly aged specimen after artificial aging for 10 hours at 175 °C. This means that there is no adverse age-hardening effect due to natural aging after artificial aging for 10 hours. It was reported that natural aging decreases the maximum hardness of the Al-Mg-Si ternary alloy,[7] but the present result suggests that additions of Cu decrease the adverse effect of natural aging to the peak hardness.

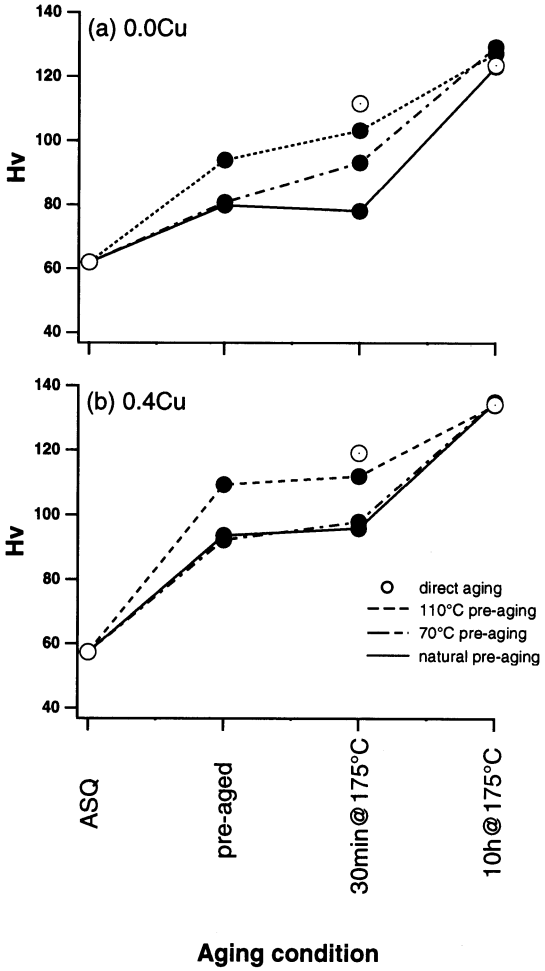

Fig. 1—Age-hardening curves of (*a*) the 0.0Cu alloy and (*b*) the 0.4Cu alloy with various preaging conditions.

Figures 2(a) and (b) show TEM bright-field images and the [001] selected-area electron diffraction (SAED) patterns obtained from the 0.0Cu alloy and 0.4Cu alloy, respectively which were aged at room temperature for 7 days (natural

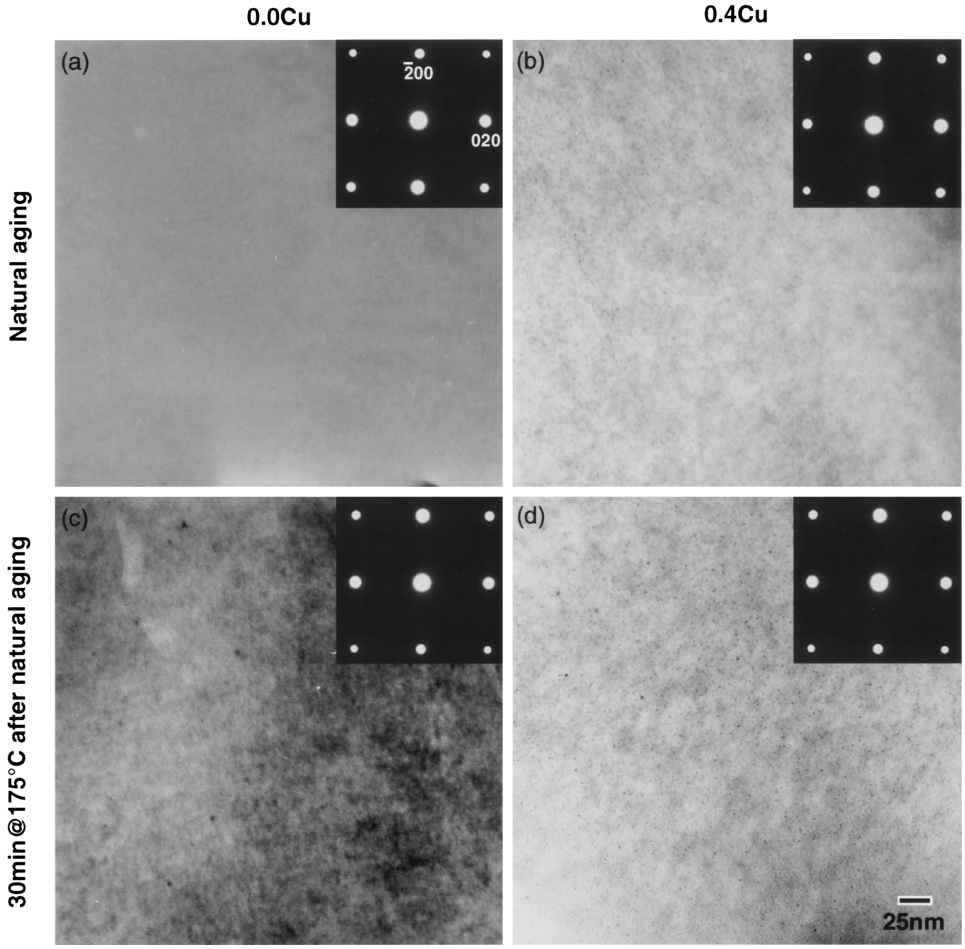

Fig. 2—TEM bright-field images of (*a*) the 0.0Cu alloy and (*b*) the 0.4Cu alloy after natural aging for 7 days, (*c*) the 0.0Cu alloy, and (*d*) the 0.4Cu alloy aged at 175 °C for 30 min after natural aging for 7 days, respectively.

aging). There is no indication of precipitate particles in the bright-field image and SAED pattern of the 0.0Cu alloy. However, a dotty contrast arising from extremely fine particles is observed in the 0.4Cu alloy, as shown in Figure 2(b). The shape of the fine precipitates is not well defined, since they are very fine (~2 nm). and the SAED pattern shows neither extra reflection nor diffuse scattering. This suggests that the precipitates are fully coherent with the matrix and do not have any distinct structure. Thus, the precipitates are designated as spherical GP zones, as was done by Dutta and Allen.[3] Figures 2(c) and (d) show TEM bright-field images and the [001] SAED patterns obtained from the 0.0Cu alloy and the 0.4Cu alloy, respectively which were artificially aged for 30 minutes after natural aging. Since the contrast due to the particles is still spherical rather than needle-shaped, and the SAED patterns show neither extra reflections nor diffuse scattering, the precipitates are designated as the spherical GP zones. The same contrast is observed in the 0.0Cu alloy, but the density of the GP zones is much lower than that in the 0.4Cu alloy, suggesting that the addition of Cu increases the density of the precipitates. These results suggest that the kinetics of precipitation in the 0.4Cu alloy appear to be faster than that in the 0.0Cu alloy.

Figures 3(a) through (c) show a series of TEM bright-field images and [001] SAED patterns obtained from the 0.4Cu alloy aged for 30 minutes at 175 °C immediately after solution treatment (directly aged), after preaging at 110 °C for 17 hours, and after preaging at 70 °C for 17 hours, respectively. In addition to the contrast due to the spherical GP zones, fine needle-shaped contrast is observed in the bright-field images of the directly aged alloy and the alloy preaged at 110 °C (Figures 3(a) and (b), respectively). In the SAED pattern shown in Figure 3(a), streaks along the ⟨001⟩ directions corresponding to the reciprocal space of the ⟨001⟩ needle-shaped precipitates are observed. According to Dutta and Allen,[3] these precipitates are designated as β''. On the other hand, only the dark contrast arising from fine spherical particles is observed in Figure 3(c), and the corresponding SAED pattern shows neither extra reflections nor diffuse scattering; these precipitates are designated as spherical GP zones.

The density of the precipitates in the artificially aged specimen after preaging at 110 °C is higher than that of the directly aged specimen, as shown in Figures 3(a) and (b). However, the hardness is higher in the directly aged specimen (Figure 1). The number density of the β'' precipitates is higher in the directly aged specimen than in the preaged specimen, which suggests that the main contributor to the hardness increase is the β'' precipitates rather than the GP zones. The density of the GP zones in the artificially aged specimens after preaging at 70 °C (Figure 3(c)) and natural aging (Figure 2(c)) is lower than that of the directly aged

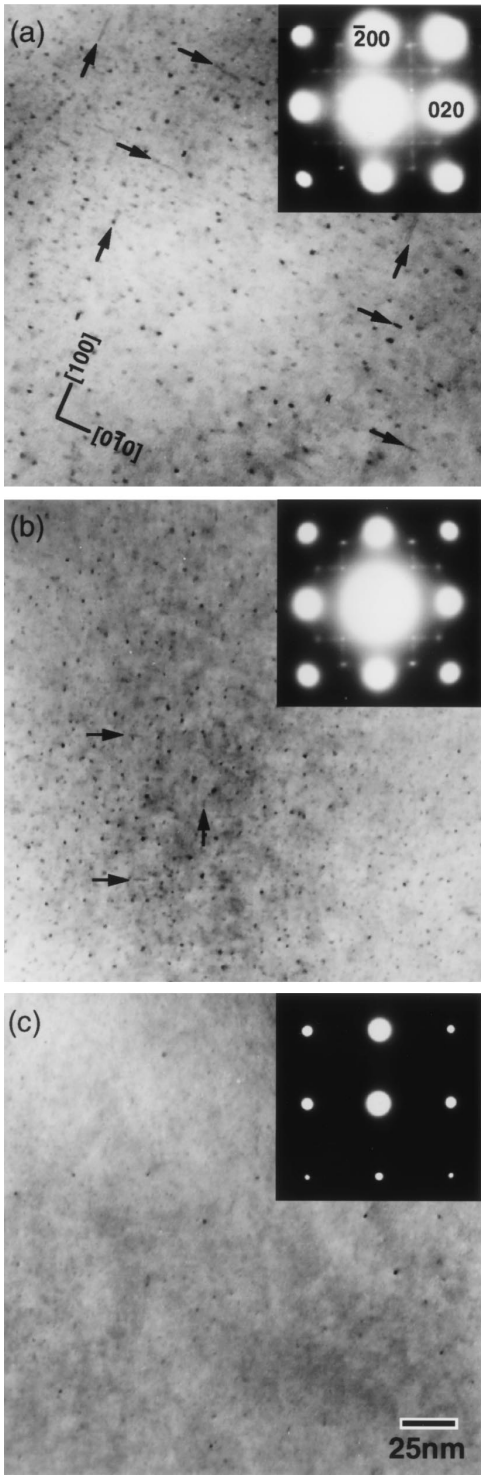

Fig. 3—TEM bright-field images and the [001] SAED patterns obtained from the 0.4Cu alloy aged at 175 °C for 30 min (*a*) after solution heat treatment and (*b*) after preaging at 110 °C for 17 h, and (*c*) after preaging at 70 °C for 17 h, respectively.

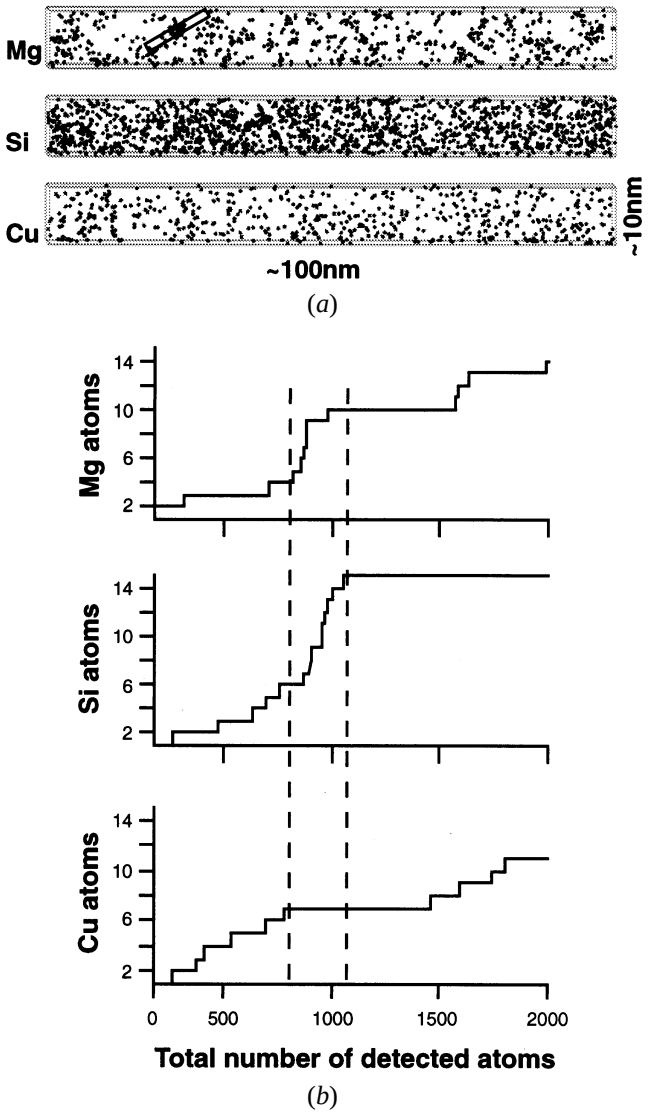

Fig. 4—(*a*) 3DAP elemental mappings of Mg, Si, and Cu atoms obtained from the 0.4Cu alloy aged at 175 °C for 30 min after preaging at 70 °C for 17h and (*b*) integrated concentration depth profiles of Mg, Si, and Cu obtained from the selected region that cover a GP zone in (a).

specimen. This is in contrast to the fact that the density of the GP zones in the artificially aged ternary Al-Mg-Si specimens after a 70 °C preaging was much higher than that in the directly aged specimen.[7]

In order to determine the chemical composition of the GP zones, 3DAP analyses have been carried out. Figure 4(a) shows 3DAP elemental mappings of Mg, Si, and Cu atoms obtained from the 0.4Cu alloy aged for 30 minutes at 175 °C after a 70 °C preaging. In these figures, individual dots correspond to the positions of individual atoms. The presence of particles enriched with Mg and Si atoms is evident from the elemental maps. However, the Cu mapping shows that the distribution of Cu atoms is rather uniform. The shape of the Mg and Si enriched particle is not well defined, and these particles are believed to correspond to the GP zones, as characterized by the TEM in Figure 3(c). Since the concentration of Mg and Si is as much as a few atomic percentages, small zones may not be visualized because they are covered in the background from the supersaturated solute atoms. Thus, a statistical method known as contingency-table analysis was employed to test whether or not there is a correlation in the distribution of Mg and Si atoms.[17] Table II shows contingency tables of the number of detected Mg and Si atoms, based on a block size of 199 atoms, for the 0.4Cu alloy aged for 30 minutes at 175 °C after a 70 °C preaging. In this table, the observed frequencies containing

Table II(a). Contingency Tables for Mg and Si Obtained from the 0.4Cu Alloy Aged for 30 Minutes at 175 °C after 70 °C Preaging

	Observed						Expected				
Mg/Si	0	1	2	≥3	Total	Mg/Si	0	1	2	≥3	Total
0	146	40	14	6	206	0	125.1	44.3	17.5	19.1	206
1	171	53	25	16	265	1	160.9	57.1	22.5	24.5	265
2	140	49	16	26	231	2	140.2	49.7	19.6	21.4	231
3	66	28	8	15	117	3	71	25.2	9.9	10.8	117
≥4	41	30	16	23	110	≥4	66.8	23.7	9.4	10.2	110
Total	564	200	79	86	929	total	564.0	200.0	79.0	86.0	929

$\chi^2 = 54.59$ with 12 deg of freedom.

Table II(b). Contingency Tables for Si and Cu Obtained from the 0.4Cu Alloy Aged for 30 Minutes at 175 °C after 70 °C Preaging

	Observed					Expected				
Cu/Si	0	1	≥2	Total	Cu/Si	0	1	≥2	Total
0	117	67	22	206	0	116.6	64.3	25.1	206
1	157	84	22	265	1	150	82.7	25.1	265
2	137	35	27	231	2	130.8	36.5	28.1	231
3	59	35	23	117	3	66.2	36.5	14.2	117
4	31	17	12	60	4	34.0	18.7	7.3	60
≥5	25	20	5	50	≥5	28.3	15.6	6.1	50
Total	526	290	113	929	Total	526.0	290.0	113.0	929

$\chi^2 = 15.15$ with 10 deg of freedom.

categorized numbers of Mg and Si atoms are tabulated. Experimentally observed frequencies and the frequencies for random distribution of Mg and Si are compared using the χ^2 test. The calculated value of χ^2 is 54.59, with 12 deg of freedom; thus, the null hypothesis that there is no correlation between Mg and Si atoms is rejected, with a significance level of 99.999 pct ($\alpha < 0.001$). The table also suggests that there is a positive correlation between the Mg and Si atoms (when Mg atoms are detected, there is a tendency for Si atoms to also be detected in the same atom block). In contrast, the analysis of the distribution of Si and Cu atoms gives the opposite result (Table II(b)). The calculated value of χ^2 is 15.15, with 10 deg of freedom. Thus, the null hypothesis that there is no correlation between the Mg and Cu atoms cannot be rejected, with a significance level of less than 95.0 pct ($\alpha > 0.05$). Figure 4(b) shows integral depth profiles or ladder plots of Mg, Si, and Cu atoms, determined from a selected volume in Figure 4(a). The number of detected solute atoms is plotted as a function of the total number of detected atoms in the volume. The horizontal axis corresponds to the depth; hence, the slope of the plots represents the local concentration of the GP zones. The number of detected Mg and Si atoms from this GP zone is 7 and 9, respectively; thus, the atomic ratio of Mg:Si in the spherical GP zone is almost 1:1. These results indicate that there is no enrichment of Cu in the GP zones, and the chemical nature of the GP zones is the same as that in the ternary Al-Mg-Si alloy with an excess amount of Si.[7,14] Therefore, it can be concluded that the addition of Cu does not change the chemical nature of the GP zones.

Figures 5(a) and (b) show TEM bright-field images and [001] SAED patterns obtained from the 0.4Cu alloy aged for 10 hours at 175 °C without preaging and after a 70 °C preaging, respectively. In both of the bright-field images, the needle-shaped strain-field contrasts are observed. In addition, the SAED patterns show streaks along the $[001]_{Al}$ and $[010]_{Al}$ directions. These streaks are from needle-shaped precipitates aligned in the $\langle 001 \rangle$ directions, which are attributed to the β'' precipitates.[18,19,20] The size and distribution of the β'' precipitates in these figures indicate that the microstructures of the specimens aged for 10 hours at 175 °C are the same regardless of the preaging conditions, although a significant difference in the density and the size of the precipitates was observed after 30 minutes of aging. These microstructural features are consistent with the hardness-measurement results, *i.e.*, the hardness becomes the same after 10 hours of aging at 175 °C, regardless of the preaging conditions.

Figure 6(a) shows 3DAP elemental maps of Mg, Si, and Cu atoms obtained from the 0.4Cu alloy aged for 10 hours at 175 °C after a 70 °C preaging. The 3DAP elemental maps of Mg and Si show the presence of needle-shaped β'' precipitates (indicated by the arrow). The needle-shaped precipitates are about 2 nm in diameter and 20 nm in length. The Cu elemental map shows that Cu is partitioned to the needle-shaped precipitates. Since the β'' precipitates are basically composed of Mg and Si, a correlation in the distributions of Cu and (Mg + Si) atoms is examined by the contingency-table analysis. Table III shows contingency tables of the Cu and (Mg + Si) atoms, based on a block size of 199 atoms, for the 0.4Cu alloy aged for 10 hours at 175 °C after a 70 °C preaging. The calculated value of χ^2 is 25.91, with 6 deg of freedom; thus, the null hypothesis that there is no correlation between the Cu and (Mg + Si) atoms is rejected, with a significance level of 99.999 pct ($\alpha < 0.001$). This result suggests that there is a positive

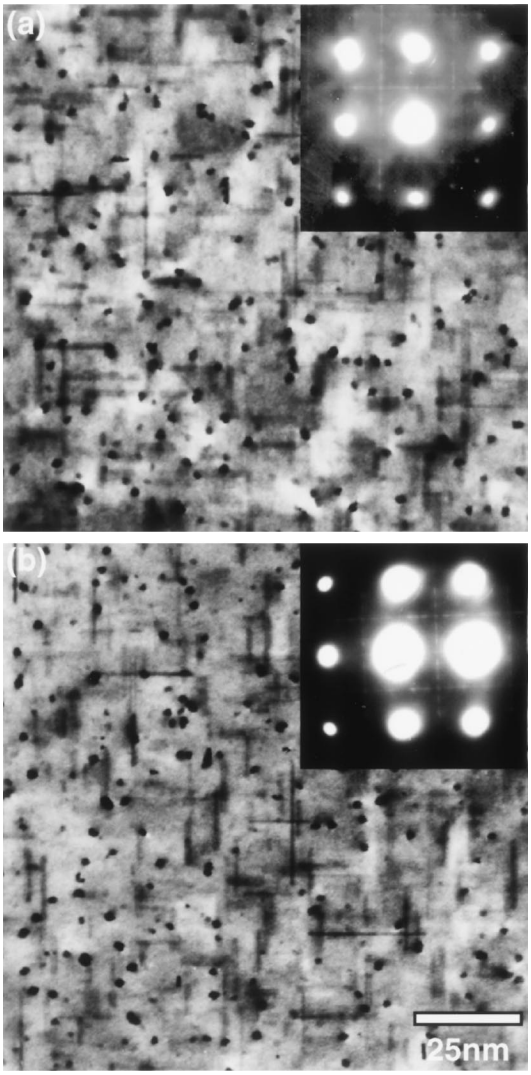

Fig. 5—TEM bright-field images and the [001] SAED patterns obtained from the 0.4Cu alloy aged at 175 °C for 10 h (*a*) after solution heat treatment, and (*b*) after a preaging at 70 °C for 17h.

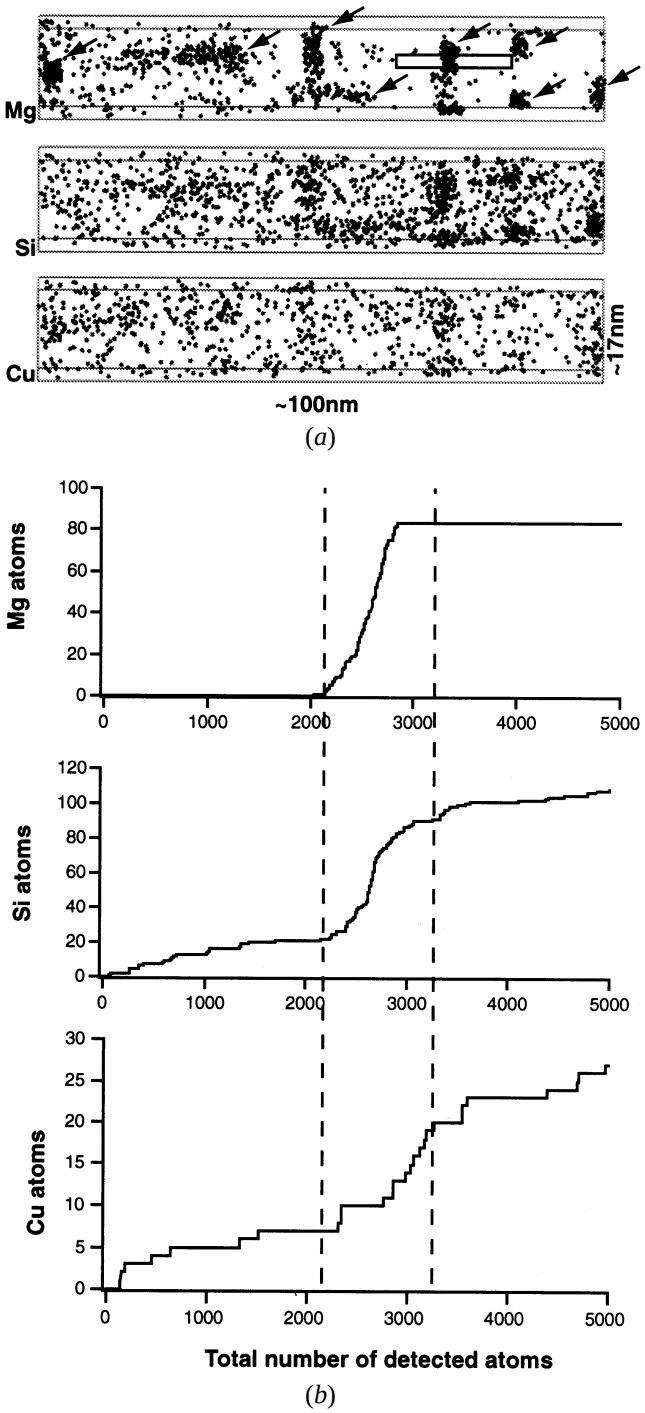

Fig. 6—(*a*) 3DAP elemental mappings of Mg, Si, and Cu atoms obtained from the 0.4Cu alloy aged at 175 °C for 30 min after preaging at 70 °C for 17 h and (*b*) integrated concentration depth profiles of Mg, Si, and Cu obtained from the selected region that cover a needle-shape β'' precipitate in Fig. (a).

correlation between Cu and the β'' precipitates. The integrated concentration-depth profiles are obtained from a needle-shaped precipitate (Figure 6(b)). The chemical composition of the needle-shaped precipitates is calculated from the slope of the plots. It has been found to be approximately 25 at. pct Mg, 25 at. pct Si, and 4 at. pct Cu, on average. Thus, it is concluded that the Cu partitioning occurs when the GP zones evolve to the β'' precipitates.

IV. DISCUSSION

The kinetics of precipitation in the directly aged 0.4Cu alloy appear to be faster than that in the preaged specimens, because a higher density of β'' precipitates are present when a specimen is aged for 30 minutes at 175 °C immediately after the solution heat treatment, whereas only GP zones are observed in the specimen aged for 30 minutes at 175 °C after preaging at lower than 70 °C. The density of the GP zones is larger in the specimen that is preaged at 110 °C, but the hardness of this specimen is lower than that of the directly aged specimen. This suggests that the precipitation of the GP zones is not very effective in hardening. Preaging at 110 °C increases the number density of the GP zones, suggesting that the preaging at 110 °C is effective in increasing the nucleation sites for the GP zones during artificial aging. This is probably because a high number density of solute clusters is formed during preaging, and these grow to GP zones without being reverted at the temperature for artificial aging. It should be noted that only GP zones were

Table III. Contingency Tables for Cu and (Mg + Si) Obtained from the 0.4Cu Alloy Aged for 10 h at 175 °C after 70 °C preaging

Observed					Expected				
Cu/Mg + Si	0	1	≥2	Total	Cu/Mg + Si	0	1	≥2	Total
0	29	21	5	55	0	27.6	17.4	10.0	55
1	32	22	5	59	1	29.7	18.6	10.0	59
2	20	8	6	34	2	17.1	10.7	6.2	34
≥3	16	10	19	45	≥3	22.6	14.2	8.2	45
Total	97	61	35	193	Total	97.0	61.0	35.0	193

$\chi^2 = 25.91$ with 6 deg of freedom.

observed after 30 minutes of aging at 175 °C in ternary alloys,[7] whereas β'' precipitates were observed in the Cu-containing alloy. Thus, we can conclude that the addition of Cu enhances the kinetics of the precipitation of β''.

Although there is no enrichment nor depletion of Cu in the GP zones, the density of GP zones in the 0.4Cu alloy artificially aged for 30 minutes after natural aging is larger than that in the 0.0Cu alloy. This trend shows good agreement with the results of the hardness measurement. The hardness values of the high-Cu alloy are always larger than those of the low-Cu alloy. In addition, the presence of GP zones in the 0.4Cu alloy is observed even after natural aging. This suggests that the increase in Cu content would increase the degree of supersaturation of Mg and Si in the alloy, which enhances the formation of clusters during natural aging. At the same time, some of the clusters evolve to the spherical GP zones. In fact, earlier electrical resistivity measurements[5,20–23] showed that the density of the solute cluster formed during natural aging becomes larger if the alloy contains larger amounts of Si or Cu.

The microstructures at the peak hardness condition show that the size and distribution of the β'' precipitates are not affected by the preaging treatments. This is in contrast to the case of the ternary alloy, where the naturally aged specimen shows a lower hardness at the peak hardness condition.[7] Thus, it is concluded that Cu negates the deterioration effect of natural aging in the peak hardness condition, but Cu does not affect the hardening after 30 minutes of aging at 175 °C. This is because the main contributor to the hardness increase is the β'' precipitate rather than the GP zones, and the formation of the β'' phase does not occur if the alloy receives natural aging before the artificial aging treatment.

It should be noted that the chemical composition of the GP zones was recorded to be much lower than that for the equilibrium Mg_2Si precipitate by 3DAP. A significant amount of Al atoms appears to be incorporated in the GP zones. However, this might be due to the artificial effect caused by the evaporation aberration that occurs when atoms are field evaporated from a locally protruding tip surface.[25] If the evaporation aberration occurs, Al atoms evaporated from the matrix are recorded within the precipitate, and the apparent chemical content of the solute in small precipitates becomes lower than the actual value. The size of the GP zones observed in the present work is approximately 2 nm in diameter, and it is possible that some Al atoms evaporated from the matrix were recorded within the precipitate volume in the position-sensitive detector of the 3DAP. However, it should also be noted that recent 3DAP investigations of small coherent particles consistently report lower solute concentrations than that of the equilibrium precipitate.[26] Since GP zones are solute-enriched clusters with coherent interfaces, the interfacial energy should be a strong function of the solute concentration. In such a case, when the particle size is small, the interfacial energy will be the dominant part of the free energy of the precipitate particle, and it might be possible that the chemical content of such small coherent zones has a great size dependency.[27] Thus, another interpretation for the present and recent 3DAP results, which report lower solute contents in fine coherent precipitates, is that the 3DAP results may reflect the actual chemical change in these coherent particles. It is very difficult to draw a conclusion at this stage as to whether or not the 3DAP data consistently give the actual composition of fine nanoscale particles; however, as far as the ratio of the solute atoms in the precipitate particles is concerned, the atom-probe data should prove to be the real value for the precipitates, as long as the overall composition determined by 3DAP is consistent with the nominal composition of the alloy. Thus, the approximate 1:1 atomic ratio of the GP zones, as well as the β'' precipitate measured in this 3DAP work, is well established. This result is consistent with recent 3DAP results which report that the solute-atom ratios in the GP zones are variable, depending on the alloy composition.[7,28] This result suggests that the GP zones are solute clusters with a highly metastable nature.

In the Cu-containing quaternary alloys, the equilibrium Q phase and its precursor phase Q', or their derivative phases, were reported.[8,10,12,13,21–24] In the present study, no indication of the presence of Q or Q' precipitates was observed even after 10 hours of aging at 175 °C. This indicates that the dominant precipitate that contributes to the peak hardness is the β'' phase rather than the Q or Q' phase. Since the Q or Q' phase precipitates at higher temperatures or after long aging times, they are not directly relevant to the age hardening in the paint-bake condition. Miao *et al.*[29] reported that the Q phase was present in the overaged condition. Since Cu is enriched in the β'' phase, it is considered that the β'' phase evolves to the Q phase after long-term aging.

V. CONCLUSIONS

Precipitation products in Al-0.61Mg-1.22Si-0.39Cu and Al-0.64Mg-1.23Si-0.03Cu alloys aged up to 10 hours at 175 °C with various preaging conditions have been characterized by TEM and 3DAP.

1. In addition to spherical GP zones, needle-shaped β'' precipitates are present in the 0.4Cu alloy aged for 30 minutes at 175 °C immediately after the solution treatment. The density of the precipitates increases when the specimen is preaged at 110 °C before artificial aging for

30 minutes at 175 °C, but the fraction of the β'' precipitate decreases, resulting in a lower hardness. Preaging at 70 °C and at room temperature causes a retardation of the precipitation kinetics, and only a lower density of GP zones is observed after artificial aging for 30 minutes. These effects of preaging disappear after artificial aging for 10 hours.
2. The spherical GP zones formed after 30 minutes of aging at 175 °C have an atomic ratio of Mg:Si atoms of close to 1:1. Cu does not associate with the formation of the GP zones.
3. Cu is enriched in the β'' precipitates that are formed after 10 hours of aging at 175 °C. Therefore, it is concluded the addition of Cu primarily enhances the formation of β'' phase during artificial aging at 175 °C.
4. No indication of the presence of Q or Q' precipitates was found up to the peak hardness. Consequently, Q and Q' precipitates do not contribute to the age hardening of this alloy at 175 °C.

ACKNOWLEDGMENTS

This work was partly supported by the New Energy Development Organization (NEDO) International Joint Research Grant. One of the authors (WFM) was supported by a grant from the Ford Motor Company.

REFERENCES

1. D.W. Pashley, J.W. Rhodes, and A. Sendorek: *J. Inst. Met.*, 1966, vol. 94, pp. 41-49.
2. G. Thomas: *J. Inst. Met.*, 1961-62, vol. 90, pp. 57-63.
3. I. Dutta and S.M. Allen: *J. Mater. Sci. Lett.*, 1991, vol. 10, pp. 323-26.
4. D.W. Pashley, M.H. Jacobs, and J.T. Vietz: *Phil. Mag.*, 1967, vol. 16, pp. 51-76.
5. S. Ceresara, E. Dirusso, P. Fiorini, and A. Giarda: *Mater. Sci. Eng.*, 1969-70, vol. 5, pp. 220-27.
6. T. Moons, P. Ratchev, P. DeSmet, B. Verlinden, and P. Van Houtte: *Scripta Mater.*, 1996. vol. 35, pp. 939-45.
7. M. Murayama and K. Hono: *Acta Mater.*, 1999, vol. 47, pp. 1537-48.
8. D.L.W. Collins: *J. Inst. Met.*, 1957-58, vol. 86, pp. 325-36.
9. D.K. Chatterjee and K.M. Entwistle: *J. Inst. Met.*, 1973, vol. 101, pp. 53-59.
10. D.E. Laughlin, W.F. Miao, L.M. Karabin, and D.J. Chakrabarti: *Automotive Alloys II*. S.K. Das, ed., TMS, Warrendale, PA, 1998, pp. 63-79.
11. H. Suzuki, M. Kanno, and Y. Shiraishi: *J. Jpn. Inst. Light Met.*, 1979, vol. 29, pp. 197-203.
12. L. Sagalowicz, G. Lapasset, and G. Hug: *Phil. Mag. Lett.*, 1996, vol. 74, pp. 57-66.
13. S.D. Dumolt, D.E. Laughlin, and J.C. Williams: *Scripta Metall.*, 1984, vol. 18, pp. 1347-50.
14. G.A. Edwards, K. Stiller, G.L. Dunlop, and M.J. Couper: *Acta Mater.*, 1998, vol. 46, pp. 3893-3904.
15. A. Cerezo, T.J. Godfrey, and G.D.W. Smith: *Rev. Sci. Instrum.*, 1988, vol. 69, pp. 49-58.
16. D. Blavette, B. Deconihout, A. Bostel, J.M. Sarrau, M. Bouet, and A. Menand: *Rev. Sci. Instrum.*, 1993, vol. 64, pp. 2911-19.
17. M.G. Hetherington, A. Cerezo, J. Hyde, G.D.W. Smith, and G.M. Worrall: *J. Phys.*, 1986. vol. 47, pp. C7-495-C7-500.
18. M.H. Jacobs: *Phil. Mag.*, 1972, vol. 26, pp. 1-13.
19. J.P. Lynch, L.M. Brown, and M.H. Jacobs: *Acta Metall.*, 1982, vol. 30, pp. 1389-95.
20. Y. Baba and A. Takashima: *J. Jpn. Inst. Light Met.*, 1969, vol. 19, pp. 90-98.
21. H. Suzuki, M. Kanno, Y. Shiraishi, and K. Hanawa: *J. Jpn. Inst. Light Met.*, 1979, vol. 29. pp. 575-81.
22. R.J. Livak: *Metall. Trans. A*, 1982, vol. 13A, pp. 1318-21.
23. G. Phragmen: *J. Inst. Met.*, 1950, vol. 77, pp. 489-552.
24. J. Crowther: *J. Inst. Met.*, 1949-50, vol. 76, pp. 201-36.
25. M.K. Miller: *J. Phys.*, 1987, vol. 48, pp. C6-565-C6-570.
26. A. Bigot, F. Danoix, P. Auger, D. Blavette, and A. Menand: *Appl. Surf. Sci.*, 1996, vol. 94-95. pp. 261-66.
27. S.R. Goodman, S.S. Brenner, and J.R. Low, Jr.: *Metall. Trans.*, 1973, vol. 4, pp. 2371-78.
28. S.K. Maloney, K. Hono, I.J. Polmear, and S.P. Ringer: *Scripta Mater.*, 1999, vol. 41, pp. 1031-38.
29. W.F. Miao and D.E. Laughlin: *Metall. Mater. Trans. A*, 2000, vol. 31A, pp. 361-71.